

## Chemical Kinetics of Hydrogen-Air-Diluent Detonations

J.E. Shepherd\*

*Sandia National Laboratories, Albuquerque, New Mexico*

### Abstract

The relationship between calculated reaction zone length and measured cell size is examined for hydrogen-air-diluent detonations. Several different means of calculating reaction zone length are discussed. A strong variation in the ratio of cell size to reaction zone length is demonstrated as a function of equivalence ratio for conventional reaction zone length definitions. A consequence of this strong variation is that single-parameter correlations can only predict cell size within  $\pm 200\%$ . A simple method for predicting cell sizes in diluted mixtures based on measured cell sizes in undiluted mixtures is suggested. This method is compared to the data for both carbon dioxide and water vapor dilution; the improved method can predict cell size within  $\pm 50\%$ . The effectiveness of  $\text{CO}_2$  and  $\text{H}_2\text{O}$  dilution in increasing the reaction zone length is shown to be due to the coupling between the thermal effect of the diluent and the chemical kinetics mechanism. The relation between initial conditions and cell size is also examined in terms of this coupling. The effect of temperature on reaction zone length is shown to also depend on pressure. Cell size predictions are compared to data for hot and cold  $\text{H}_2$ -air detonations.

### Introduction

Detailed reaction kinetics modeling has become an accepted technique for estimating dynamic detonation parameters. These

---

Presented at the 10th ICDERS, Berkeley, California, August 4-9, 1985. This paper is declared a work of the U.S. Government and therefore is in the public domain.

\*Member of the Technical Staff, Fluid and Thermal Sciences Department.

parameters include cell size, critical tube diameter, and initiation energy. Due to the lack of a quantitative theory, the relationships between calculated reaction zone length and the dynamic parameters are purely empirical. One example of such an empirical correlation is the relation proposed by Westbrook and Urtiew (1983) between cell size  $\lambda$  and reaction zone length  $\Delta$  at stoichiometric conditions:  $\lambda \simeq 20\Delta$  for fuel-air mixtures; and,  $\lambda \simeq 35\Delta$  for fuel-oxygen mixtures.

While these estimates are useful guidelines, our understanding of the relationship between cellular structure and kinetics is still quite vague and the a priori prediction of cell size is not yet possible. The empirical correlation mentioned above is just a guideline and has never been extensively tested in a quantitative fashion. Comparison between the computed reaction zone lengths (Westbrook and Urtiew 1982) and recent cell size data (Moen et al. 1984a) indicates that the ratio of cell size to reaction zone length varies between 10 and 50 for many common fuel-air mixtures at stoichiometric composition. The present research and previous studies by Strehlow et al. (1969a) show that the ratio is a strong function of the equivalence ratio  $\phi$  and the particular definition of reaction zone length used. For off-stoichiometric mixtures, the ratio of measured cell size to reaction zone length can vary between 2 and 100. The variation is strongest near the rich and lean limits, usually regions of great interest in explosive hazards evaluations. In addition to these variations, there is an associated uncertainty in the measured cell size due to the very irregular cellular structure of fuel-air mixtures (Moen et al. 1984a; Bull et al. 1982).

Recent developments in detonation research (Lee 1984) have suggested that cell size is the single fundamental parameter that can be simply related to both critical tube diameter and initiation energy. Given this increasing emphasis on cell size and the empirical nature of our predictive ability, it is important to understand the limitations of using chemical kinetics modeling and empirical correlations to predict cell size. We have attempted to do that for  $H_2$ -air-diluent detonations using the substantial amount of experimental data on cell sizes. Many of these data have been taken by researchers at McGill University and Sandia National Laboratories, Albuquerque (SNLA), during the last four years (Guirao et al. 1982; Tieszen et al. 1985). This research has been directed at understand-

ing the detonability of  $H_2$ -air-steam mixtures that might occur as a result of a hypothetical degraded-core accident in a nuclear reactor.

The present report will concentrate on the problem of predicting cell size for the hydrogen-air-diluent system. Following a historical perspective on the general problem of predicting cell size, specific results for the  $H_2$ -air system are discussed. Several definitions of reaction zone length and the resulting correlation with measured cell size are examined. A technique for predicting cell sizes in diluted mixtures, given the cell size in undiluted mixtures, is discussed. Comparisons between predictions and data are shown for both carbon dioxide and water vapor dilution. This work is a consolidation and extension of earlier efforts (Lee et al. 1982; Shepherd and Roller 1982) and, hopefully, will make our results more accessible to the combustion research community. The effect of dilution and changing initial conditions on the reaction zone length are interpreted in terms of the coupling between thermal and chemical kinetics phenomena.

### Historical Perspective

Detonation cellular structure and the possibility of a priori computations of cell size has intrigued researchers since the discovery of this fascinating phenomenon. Previous theoretical and experimental efforts devoted to this problem have provided many important facts and ideas that the present paper draws upon. Shchelkin and Troshin (1965) first attempted to relate the calculated steady-state reaction zone length to the observed cellular structure for detonations in hydrogen-, heptane-, and benzene-oxygen mixtures. They proposed the linear proportionality relationship that is frequently used today.

Using a heuristic argument based on acoustic wave propagation of disturbances in a square-wave model reaction zone, they attempted to compute the coefficient of proportionality. They found that the cell width should be approximately four times the induction zone length used in the square-wave model. Like present researchers, they had to confront the problem of irregularity and chose a single length scale from the observed spectrum of sizes. However, at that time (1959), the state of knowledge about the oxidation mechanisms and rate constants was so uncertain that the prediction could not

be tested. Instead, they used the argument in reverse to attempt to compute activation energies from the measured cell size.

The relation between cell size and reaction zone lengths in fuel-oxygen mixtures was extensively investigated by Strehlow et al. (1969a), Strehlow and Engels (1969b), and Strehlow (1969c). These studies convincingly demonstrated that the dominant factor in determining cell size was indeed the reaction zone length. However, the observations showed a complex dependence of the cell size on reaction zone length, initial pressure, diluent fraction and stoichiometry.

The most detailed studies of Strehlow and co-workers were performed with  $H_2$ - $O_2$  mixtures diluted with various inert gases. Comparison was made between measured cell sizes and reaction zone structures computed from the ZND model and relatively detailed chemical kinetic mechanisms. These comparisons indicated that when the induction zone became large compared to the recombination zone, the cell size was directly proportional to the induction zone length. For large enough initial pressure, the constant of proportionality was essentially independent of pressure for fixed mixture composition. The constant was found to vary strongly with both the equivalence ratio (from 70 to 170 for  $H_2$ - $O_2$  diluted with 40% Ar) and the amount and type of diluent (from 60 to 120 for 0% to 80% Ar dilution of stoichiometric  $H_2$ - $O_2$ ). For a given induction time, the cell size was proportional to the postshock sound speed for monatomic diluents. When the induction zone became short compared to the recombination zone, no simple correlations could be determined.

Contemporaneous with these experimental investigations, Erpenbeck (1969) rigorously analyzed the linear stability of steady detonations to arbitrary three-dimensional disturbances. Unfortunately, the resulting system of equations is so complex that no explicit dispersion relation is available as a guide for correlating experimental data with kinetic parameters. He did obtain results for the stability boundaries in the short- and long-wavelength limits for a one-step Arrhenius reaction rate model. The only predictions of fully developed instability wavelength were made for the longitudinal (one-dimensional) mode of marginally unstable systems.

Strehlow and co-workers (Strehlow and Fernandes 1965; Barthel and Strehlow 1966) developed an alternative approximate analysis based on geometrical acoustics that demonstrated the trapping of nonreactive acoustic waves within the reaction zone. The trapped



wavefronts originating at the shock rapidly become convoluted and the wavefront folds contact the shock with a regular spacing. Computed shock-contact spacings were of the same order of magnitude as the reaction zone thickness and one to two orders of magnitude smaller than the observed cell widths.

An extension of this analysis by Barthel (1974) demonstrated the production of periodic caustics by trapped waves originating inside the reaction zone; the computed caustic spacing was a factor of 1.7–2.5 larger than the observed transverse wave spacings for the  $\text{H}_2\text{-O}_2$  system. The trapped waves exhibit a range of ray transit times between turning points with a minimum value corresponding to the caustic spacing. Using this fact, Chiu and Lee (1976) demonstrated that Barthel's model could be simplified dramatically for square-wave model reaction zones and arrived at the conclusion that the caustic spacing was linearly proportional to the reaction zone length with a constant of about 6 for typical fuel-oxygen systems. The constant of proportionality only depends on the detonation Mach number and the cold gas specific heat ratio. Both versions of this model have only been tested against data for the  $\text{H}_2\text{-O}_2\text{-Ar}$  system at stoichiometric conditions. The results exhibit the correct pressure dependence but almost any model based on reaction zone length can do that.

However, all of these theoretical approaches suffer several common deficiencies. They are perturbation methods that ignore three important aspects of the problem: the finite amplitude of the transverse waves; coupling between transverse waves and the main shock wave; reaction behind the transverse waves. In addition, all methods except Barthel's use an approximate model of the reaction zone or reaction mechanism and no prescription has been given for generating the model parameters corresponding to realistic fuel-oxidizer systems.

Experimentally, the transverse waves and the main shock (detonation) wave are observed to be very strongly coupled. This results in finite amplitude oscillations in both transverse and longitudinal shock strength. The longitudinal oscillations are due both to the gas-dynamic coupling of the main shock with the transverse waves and the intrinsic longitudinal instability of a one-dimensional detonation wave. The variation in shock wave strength through the cell and the nonlinear coupling of reaction rates to the gas thermodynamic state

results in a large variation in reaction zone length through the cell. For example, the main shock wave velocity in ordinary detonations varies from about  $1.2 U_{CJ}$  at the beginning of the cell to  $0.8 U_{CJ}$  at the end. The equivalent steady-state induction time for a stoichiometric hydrogen-air mixture initially at standard conditions varies from  $1.2 \times 10^{-7}$  s to  $3.4 \times 10^{-4}$  s, a range of  $10^3$ . This means that the assumed steady-state reaction zone structure does not exist and perturbation analyses about this fictitious state will not yield quantitative predictions. The studies mentioned above have all recognized this fact, but the coupled problem still eludes solution.

Interesting alternative methods that do not suffer these deficiencies are based on the similarity of the main shock motion to that of a self-similar decaying blast wave. The source of the blast is the nearly-simultaneous explosion of the "pocket" of unreacted fluid located at the end of the cell. The explosion is initiated by the collision of the transverse waves. The geometrical structure of the cell and the wave fields are essentially universal, i.e., independent of the fuel-oxidizer system. An absolute length scale is determined by the point at which the reaction zone decouples from the main shock wave.

At the present time, the best example of this genre is the model of Vasiliev and Nikolaev (1978) for planar mode (two-dimensional) detonations. They show good agreement between predicted cell shapes and cell lengths as a function of initial pressure for stoichiometric methane-, acetylene-, and hydrogen-oxygen mixtures. As pointed out above, this does not constitute a very rigorous test of the model. These comparisons use both an approximate model of the reaction zone and simple one-step correlations for the induction time, and it is not obvious how to generalize this approach to include more realistic reaction kinetics. In addition, the model is for two-dimensional cellular structures but is applied to problems where the known structure is fully three-dimensional.

Recent efforts in the field (including the present paper) have concentrated on improving the treatment of the chemical kinetics portion of the problem and have ignored the gasdynamics and multidimensional nature of the observed cellular structure. For simplicity, an empirical approach is used in which the reaction zone length is assumed to be the fundamental scaling length that is empirically related to the measured detonation parameters. Using very detailed

reaction mechanisms, Westbrook and Urtiew (1982, 1983) have carried out the most extensive program of reaction zone computation and correlation with measured dynamic detonation parameters for a wide variety of hydrocarbon fuels.

While some cell size data were examined, they mainly concentrated on the prediction of critical tube diameters and direct initiation energy. Cell size for stoichiometric methane-, acetylene-, and hydrogen-oxygen mixtures was examined as a function of initial pressure. Good agreement between predicted and measured cell size was obtained with an average coefficient of proportionality equal to 29. No direct comparison was given for fuel-air mixtures. Previous studies (Westbrook 1982) considering off-stoichiometric and diluted fuel-oxygen mixtures found a considerable variation in the ratio of cell size to reaction zone length.

In addition to the studies mentioned above that directly bear on the problem of cell size prediction, there are many other reports dealing with related problems. In particular, there have been several numerical simulations of marginal (single-mode) detonations in one† and two dimensions (Oran et al. 1982; Taki and Fujiwara 1982). These studies indicate that if a single mode is present in the system and the reaction mechanism can be condensed to a simple parametric model, time-dependent computations may be possible for computing the cell size. No general conclusions applicable to ordinary systems can be drawn from these studies except that the multimode structure of typical fuel-air systems may make the computations exceedingly difficult.

In summary, despite a number of efforts over the last two decades, the problem of detonation cell size prediction remains unsolved. No single theory presently exists containing the appropriate multidimensional gasdynamics, realistic reaction kinetics, and the finite amplitude waves observed experimentally. Most models have only been tested against stoichiometric fuel-oxygen mixture data primarily as a function of initial pressure. Appropriate choice of the model parameters can be made to obtain agreement for almost any model. A much more rigorous test for modelers is to predict the

---

†See Fickett and Wood (1966), Howe et al. (1976), and Moen et al. (1984a).

cell size as a function of equivalence ratio, dilution, and initial pressure.

### Reaction Zone Computation

The idealized, one-dimensional, Zeldovich, von Neumann, and Döring (ZND) model of detonation is used to calculate the reaction zone structure. A reactionless shock wave traveling at the Chapman-Jouguet (CJ) velocity is assumed to instantaneously raise the fluid temperature and pressure and to initiate chemical reaction. The equations for fluid pressure, density, and composition are simultaneously integrated as a function of distance (or time) behind the shock wave. The fluid state proceeds down the Rayleigh line from the von Neumann (VN) point (no reaction) toward the CJ point (complete reaction).

Detonation velocities used in these computations were calculated by the NASA chemical equilibrium code (Gordon and McBride 1971). The reaction zone structure was computed by a program developed especially for this project. In addition to the ZND structure, computations were also performed with the commonly used constant-volume approximation to the Rayleigh line for some cases.

A set of 23 reactions and 11 species ( $H_2$ ,  $O_2$ ,  $H$ ,  $O$ ,  $OH$ ,  $H_2O$ ,  $HO_2$ ,  $H_2O_2$ ,  $N_2$ ,  $CO_2$ , and  $CO$ ) are used in the kinetic model for hydrogen oxidation. The reaction mechanisms and rate constants are given in Table 1. Only forward rates are listed, but all reactions were considered completely reversible in the computations. Reverse rates are obtained from the forward rates and the equilibrium constants. Rate constants were obtained from Miller et al. (1982).

Several definitions of reaction zone length have been considered in the present work. All of these lengths are measured from the shock wave in the frame of reference moving with the shock. Three lengths are based on the ZND structure and two on the constant-volume approximation to the Rayleigh line. These lengths are defined in Table 2. Numerical values for a stoichiometric  $H_2$ -air detonation at standard initial conditions are given in the Table 2 and are also indicated on the temperature profile shown in Fig. 1. For reference, the major and minor species profiles are shown in Figs. 2 and 3. The meanings of the various length scales are discussed below.

Length  $\Delta_1$  is a conventional induction zone length that approximately measures the extent of the thermally neutral portion

Table 1 Hydrogen oxidation mechanism and rate constants<sup>a</sup>

Reaction	A	$\beta$	E
1. $\text{H}_2 + \text{O}_2 \rightleftharpoons \text{OH} + \text{OH}$	$1.70 \times 10^{13}$	0.00	47780
2. $\text{OH} + \text{H}_2 \rightleftharpoons \text{H}_2\text{O} + \text{H}$	$1.17 \times 10^9$	1.30	3626
3. $\text{H} + \text{O}_2 \rightleftharpoons \text{OH} + \text{O}$	$5.13 \times 10^{16}$	-0.82	16507
4. $\text{O} + \text{H}_2 \rightleftharpoons \text{OH} + \text{H}$	$1.80 \times 10^{10}$	1.00	8826
5. $\text{H} + \text{O}_2 + \text{M} \rightleftharpoons \text{HO}_2 + \text{M}$	$2.10 \times 10^{18}$	-1.00	0
6. $\text{H} + \text{O}_2 + \text{O}_2 \rightleftharpoons \text{HO}_2 + \text{O}_2$	$6.70 \times 10^{19}$	-1.42	0
7. $\text{H} + \text{O}_2 + \text{N}_2 \rightleftharpoons \text{HO}_2 + \text{N}_2$	$6.70 \times 10^{19}$	-1.42	0
8. $\text{OH} + \text{HO}_2 \rightleftharpoons \text{H}_2\text{O} + \text{O}_2$	$5.00 \times 10^{13}$	0.00	1000
9. $\text{H} + \text{HO}_2 \rightleftharpoons \text{OH} + \text{OH}$	$2.50 \times 10^{14}$	0.00	1900
10. $\text{O} + \text{HO}_2 \rightleftharpoons \text{O}_2 + \text{OH}$	$4.80 \times 10^{13}$	0.00	1000
11. $\text{OH} + \text{OH} \rightleftharpoons \text{O} + \text{H}_2\text{O}$	$6.00 \times 10^8$	1.30	0
12. $\text{H}_2 + \text{M} \rightleftharpoons \text{H} + \text{H} + \text{M}$	$2.23 \times 10^{12}$	0.50	92600
13. $\text{O}_2 + \text{M} \rightleftharpoons \text{O} + \text{O} + \text{M}$	$1.85 \times 10^{11}$	0.50	95560
14. $\text{H} + \text{OH} + \text{M} \rightleftharpoons \text{H}_2\text{O} + \text{M}$	$7.50 \times 10^{23}$	-2.60	0
15. $\text{H} + \text{HO}_2 \rightleftharpoons \text{H}_2 + \text{O}_2$	$2.50 \times 10^{13}$	0.00	700
16. $\text{HO}_2 + \text{HO}_2 \rightleftharpoons \text{H}_2\text{O}_2 + \text{O}_2$	$2.00 \times 10^{12}$	0.00	0
17. $\text{H}_2\text{O}_2 + \text{M} \rightleftharpoons \text{OH} + \text{OH} + \text{M}$	$1.30 \times 10^{17}$	0.00	45500
18. $\text{H}_2\text{O}_2 + \text{H} \rightleftharpoons \text{HO}_2 + \text{H}_2$	$1.60 \times 10^{12}$	0.00	3800
19. $\text{H}_2\text{O}_2 + \text{OH} \rightleftharpoons \text{H}_2\text{O} + \text{HO}_2$	$1.00 \times 10^{13}$	0.00	1800
20. $\text{HO}_2 + \text{CO} \rightleftharpoons \text{CO}_2 + \text{OH}$	$1.51 \times 10^{13}$	0.00	22934
21. $\text{CO} + \text{O} + \text{M} \rightleftharpoons \text{CO}_2 + \text{M}$	$3.20 \times 10^{13}$	0.00	-4200
22. $\text{CO} + \text{OH} \rightleftharpoons \text{CO}_2 + \text{H}$	$1.51 \times 10^7$	1.30	-758
23. $\text{CO} + \text{O}_2 \rightleftharpoons \text{CO}_2 + \text{O}$	$1.60 \times 10^{13}$	0.00	41000

<sup>a</sup>Reaction rate coefficients are in the form  $k_f = AT^n \exp -E/RT$ . Units are moles, cubic centimeters, seconds, Kelvins, and calories/mole.

Third body efficiencies:  $k_5(\text{H}_2\text{O}) = 21k_5(\text{Ar})$ ;  $k_5(\text{H}_2) = 3.3k_5(\text{Ar})$ ;  $k_5(\text{CO}_2) = 5k_5(\text{Ar})$ ;  $k_5(\text{CO}) = 2k_5(\text{Ar})$ ;  $k_{12}(\text{H}_2\text{O}) = 6k_{12}(\text{Ar})$ ;  $k_{12}(\text{H}) = 2k_{12}(\text{Ar})$ ;  $k_{12}(\text{H}_2) = 3k_{12}(\text{Ar})$ ;  $k_{14}(\text{H}_2\text{O}) = 20k_{14}(\text{Ar})$ .

of the reaction zone. This length is determined by the point of the maximum temperature gradient in the reaction zone, which corresponds to the point of maximum heat release rate. Length  $\Delta_3$  is determined by the point at which the Mach number (in a shock-fixed frame) reaches 0.90 and is indicative of the total length of the reaction zone, induction plus recombination zones. The length  $\Delta_2$  is determined by the point at which the Mach number reaches 0.75 and is an intermediate scale that appears to be most successful in predicting the change of cell size with dilution.



Table 2 Reaction zone lengths

Symbol	Definition	Values at $\phi = 1$	
		$\Delta$ , cm	$\lambda/\Delta$
ZND model			
$\Delta_1$	$\frac{dT}{dx} _{\max}$	0.023	65.
$\Delta_2$	$M = 0.75$	0.067	22.
$\Delta_3$	$M = 0.90$	0.43	3.5
Constant-volume model			
$\Delta_4$	$\frac{dT}{dx} _{\max}$	0.021	71.4.
$\Delta_5$	$= -T_{vn} \frac{\partial \Delta_4}{\partial T_{vn}} _{\rho}$	0.173	8.6

$M$  = Mach number.  $\Delta$  = reaction zone length.  $\lambda(\phi = 1) = 1.5$  cm for  $H_2$ -air mixtures initially at STP.

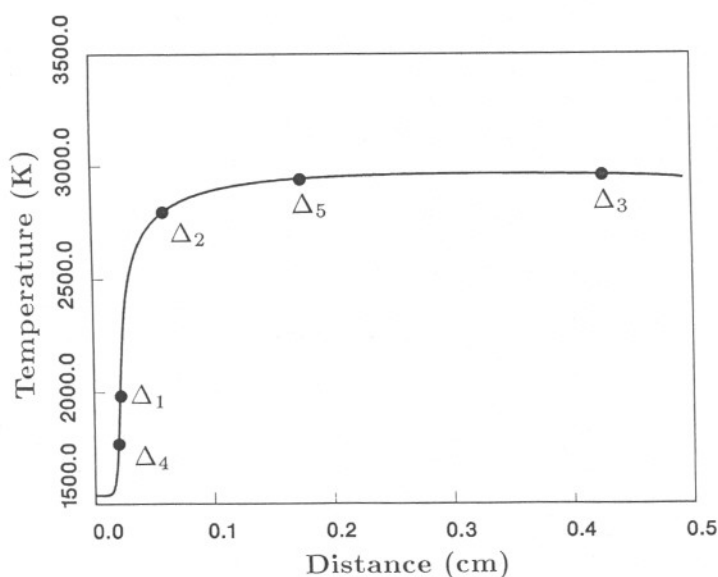


Fig. 1 ZND reaction zone temperature profile for a stoichiometric  $H_2$ -air detonation (standard initial conditions,  $T_o = 298$  K and  $P_o = 1$  atm).

Length  $\Delta_4$  is the analog of  $\Delta_1$  for the constant-volume model. Westbrook and Urtiew have used  $\Delta_4$  in their extensive discussions (Westbrook and Urtiew 1982, 1983; Westbrook 1982) of hydrocarbon-air detonations. Note that in the constant-volume approximation, distance is computed as  $\Delta = ut$ , where  $u$  is the (fixed) postshock fluid velocity and  $t$  is the Lagrangian time. Values of  $\Delta_1$  and  $\Delta_4$

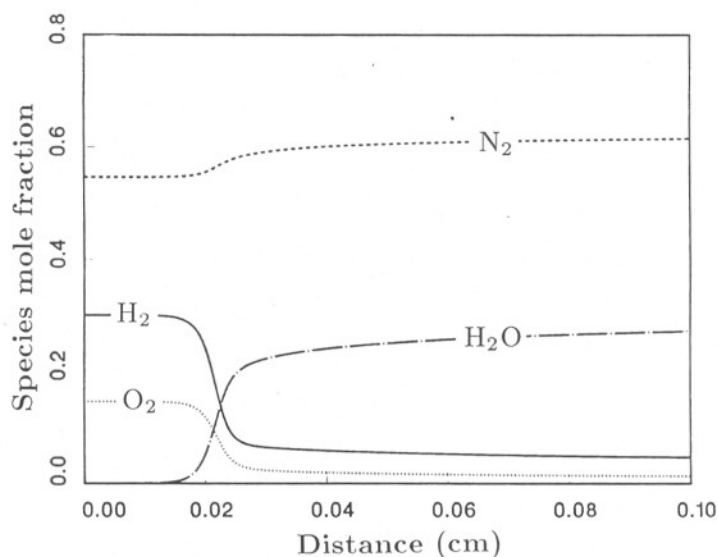


Fig. 2 Major species profiles for the detonation described in Fig. 1.

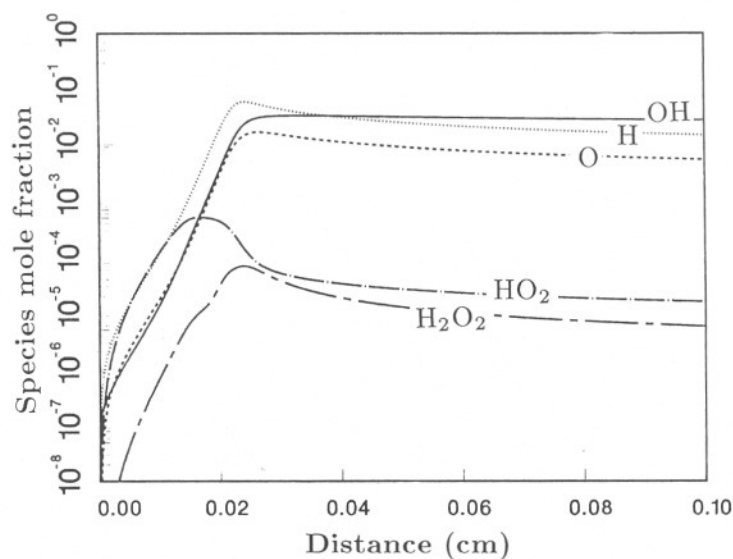


Fig. 3 Minor species profiles for the detonation described in Fig. 1.

are very similar despite the different coupling between the chemistry and fluid dynamics in the two models. Calculations with a constant-pressure model of the reaction zone also yields values of  $\Delta$  that are almost identical to  $\Delta_1$  and  $\Delta_4$ .

Length  $\Delta_5$  is related to the effective activation energy  $E$ ,

$$\frac{\Delta_5}{\Delta_4} = -\frac{T_{vn}}{\Delta_4} \left. \frac{\partial \Delta_4}{\partial T_{vn}} \right|_p = \frac{E}{RT_{vn}};$$

where I have assumed that the induction time  $t_{\text{ind}}$  can be described by a single-step or global expression of the form

$$t_{\text{ind}} = C[\text{H}_2]^\alpha [\text{O}_2]^\beta \exp(E/RT_{\text{vn}}),$$

for small variations in  $T_{\text{vn}}$ . This type of simple expression, although limited in applicability, is very useful for understanding the effect of dilution and changing initial conditions on the reaction zone length. Typical values used for hydrogen-oxygen systems are  $C = 6.9 \times 10^{-11}$ ,  $\alpha = 0$ ,  $\beta = -1$ , and  $E = 16.5$  kcal/mole. Moen et al. (1984a) deduced an effective activation energy of approximately 32 kcal/mole from fits to cell size or critical tube diameter data. This value is consistent with the average of the values derived (see the discussion below and Fig. 6) from the present computations. Numerically, the values of  $\Delta_5$  and  $\Delta_3$  are quite similar and both are a factor of 5-10 larger than the values of  $\Delta_1$ ,  $\Delta_2$ , and  $\Delta_4$ .

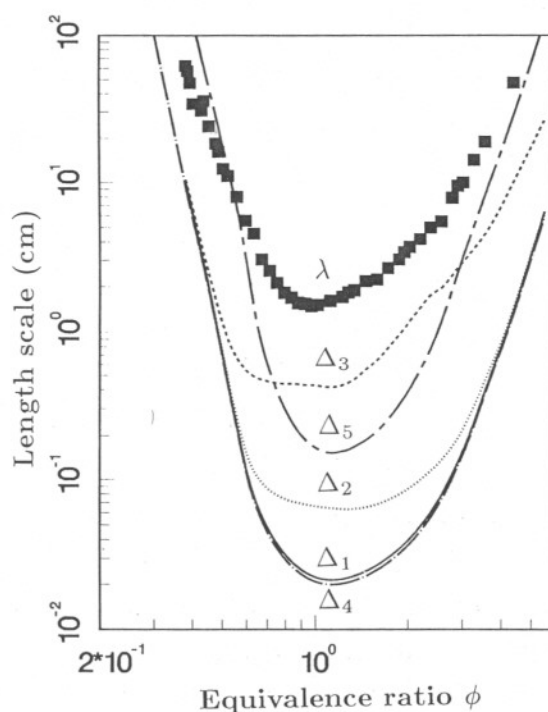


Fig. 4 Cell size  $\lambda$  and reaction zone lengths  $\Delta_1 - \Delta_5$  for  $\text{H}_2$ -air detonations (standard initial conditions).

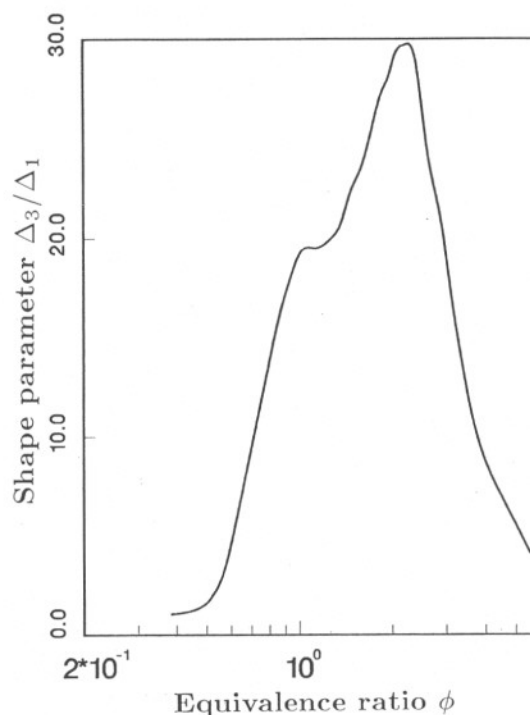


Fig. 5 Shape parameter,  $\Delta_3/\Delta_1$  vs equivalence ratio for  $H_2$ -air detonations (standard initial conditions).

### $H_2$ -Air Detonations

The values of each  $\Delta$  have been computed for  $H_2$ -air detonations over an equivalence ratio<sup>‡</sup> range of  $0.38 \leq \phi \leq 5.56$  (13% -70%  $H_2$  by volume) for standard initial conditions,  $T_o = 298$  K and  $P_o = 1$  atm. The results of those calculations are shown in Fig. 4 together with the cell size data of both Sandia and McGill. Away from the limits, i.e., for  $0.7 \leq \phi \leq 3$ , there is a large spread in the values of the various  $\Delta_i$ . This is due to the importance of the recombination zone in determining the total reaction zone length for these cases.

As the mixture is changed from stoichiometric conditions, the induction zone length increases much more rapidly than does the recombination zone length (which is essentially constant), and the various  $\Delta_i$  become comparable in magnitude. This indicates that the shape of the reaction zone can change significantly with equivalence

<sup>‡</sup>I define the equivalence ratio  $\phi$  to be the ratio of moles of fuel to moles of oxidizer divided by that ratio at stoichiometric conditions.

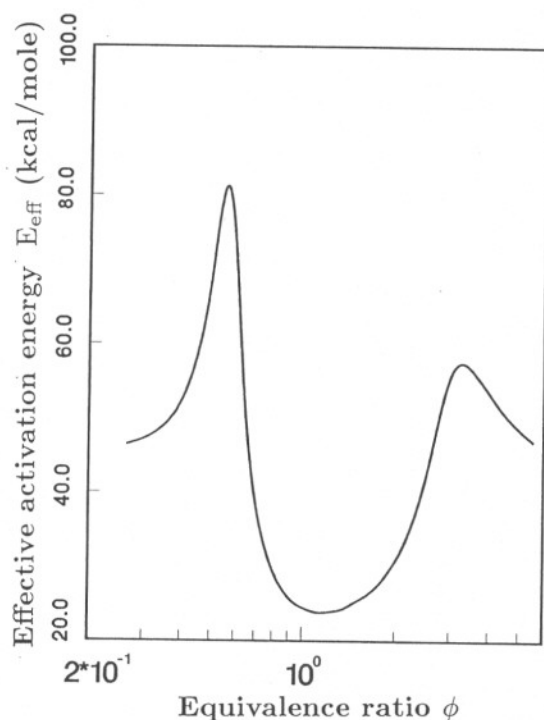


Fig. 6 Effective activation energy vs equivalence ratio for  $\text{H}_2$ -air detonations (standard initial conditions).

ratio and is a much more important factor at  $\phi = 1$  than near the limits. One quantitative measure of the shape is the ratio of total reaction zone length to induction zone length,  $\Delta_3/\Delta_1$ , plotted in Fig. 5. Note that only at the far extremes of the equivalence ratio range does the induction zone dominate totally. This behavior makes it difficult to approximate the reaction zone with the simple square-wave model used in many analyses.

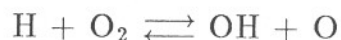
An indication of the insensitivity of the reaction zone length to computational technique can be seen by comparing the  $\Delta_1$  and  $\Delta_4$  curves in Fig. 4. For this length scale, very little effect of the thermodynamic path is seen. This is because the thermally neutral portion of the reaction dominates the determination of these lengths except near stoichiometric conditions. Computations with other sets of rate constants (Warnatz 1984; Westbrook and Dryer 1984) result in almost identical results to those shown in Fig. 4. The primary difference between the mechanisms is the rate of the three-body reaction (9), which can have a value that is a factor of 20 higher with  $\text{H}_2\text{O}$  as the diluent rather than  $\text{N}_2$ ,  $\text{O}_2$ , or Ar. Differences in computed reaction zone lengths due to reaction rates or computation



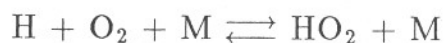
method appear to be insignificant in view of the large and often unquantified uncertainties in measured cell size.

There is no evidence in the present calculations of any intrinsic limit to detonability due to a drastic change in reaction mechanism at some limiting value of  $\phi$ . For example, a well-defined reaction zone is found to exist at an equivalence ratio as low as 0.2 (8%  $\text{H}_2$ ). The reaction zone length increases rapidly as the equivalence ratio is decreased (increased) at the lean (rich) extreme but there is no "discontinuity" in this dependence. The ability to initiate or propagate a detonation near the rich or lean limits appears to be determined by the same factors that are important for nonlimit mixtures, e.g., the size of the apparatus and the strength of the initiator.

Belles (1959) first proposed such a limit in analogy to the classical second explosion limit observed in low-temperature combustion bomb experiments. That limit is due to the competition between the chain-branching reaction 3,



and the three-body reactions 5-7,



In vessel explosions, the experiment duration is quite long compared to the characteristic species diffusion time and the relatively stable species  $\text{HO}_2$  is lost to the vessel walls. Therefore, the competition for H atoms results in chain breaking by reactions 5-7, effectively inhibiting the explosion.

In detonations, diffusion is usually negligible and, as is now well known (Westbrook and Dryer 1984),  $\text{HO}_2$  reacts with either H (reaction 9) to directly produce OH or with itself (reaction 16) to produce  $\text{H}_2\text{O}_2$  which dissociates (reaction 17) to produce OH. Ultimately, the  $\text{HO}_2$  is consumed and the standard chain branching involving OH dominates at the end of the reaction zone. It is apparent that  $\text{HO}_2$  and  $\text{H}_2\text{O}_2$  are vitally important in determining the reaction zone structure near the limits. Even for stoichiometric  $\text{H}_2$ -air detonations, a substantial amount of  $\text{HO}_2$  is observed in the beginning of the reaction zone (see Fig. 3).

More recently, Atkinson et al. (1980) proposed limits of  $\phi = 0.35 - 0.40$  and  $\phi = 5.5 - 6.0$  based on drastic changes in the radical populations outside these limits. This behavior was observed in detailed kinetic simulations using a constant-pressure model of the reaction zone. No such behavior has been observed in our ZND or constant-volume calculations. Apparently, this contradiction is due to some differences in the kinetic mechanism and the use of the different reaction zone models. The existence of an intrinsic detonability limit is obviously an unresolved issue.

Despite the uncertain status of an intrinsic limit, the competition for H atoms between reactions 3 and 5-7 is still very significant. The present interpretation of the significance is that near the limits, the principal rate-controlling reaction changes, with a corresponding change in the effective activation energy. A plot of computed effective activation energy vs equivalence ratio is shown in Fig. 6. The present calculations indicate that near stoichiometric conditions, the effective activation energy is a minimum,  $E \approx 24$  kcal/mole.

This is higher than the activation energy of 16.5 kcal/mole for the usual rate-limiting step 3 due to the importance of the competing three-body reactions 5-7. As the limits are approached, the value increases to a maximum of 50-80 kcal/mole, then drops down to a value of  $\sim 45$  kcal/mole at the extremes of the equivalence ratio range. The value reached at the rich or lean limits is consistent with reaction 17 being the rate-limiting step at the very rich or lean extremes. The large changes observed in  $E$  near the limits suggests that extrapolating cell size with a simple global reaction time formula will not be reliable. These results can also have strong implications for interpreting the effects of diluents and changing initial conditions, as discussed below.

### Cell Size Prediction

How can these reaction zone lengths be used to predict cell size? In view of the difficulties with the theoretical approaches discussed above, I have reverted to the simplest possible technique for predicting cell size. This method is similar to the original suggestion (Shchelkin and Troshin 1965) that the cell size is simply proportional to the reaction zone length. Unlike the previous studies discussed above, no attempt is made to compute the coefficient of proportionality, but it is treated as an empirically determined factor. This

method is obviously not a scientific but rather an empirical approach to the problem of cell size prediction. Such a technique will never replace a comprehensive theoretical model of detonation instability and cellular structure.

The simplest empirical approach is to use a single constant  $A_i$  and to estimate cell size by the simple linear relation  $\lambda = A_i \Delta_i$ . The value of  $A$  is usually determined by matching  $\Delta$  and  $\lambda$  at a single point, often stoichiometric composition. Values of  $A_i$  for a stoichiometric mixture of  $H_2$ -air are given in Table 2; these range from 3.5 for  $A_3$  to 71.4 for  $A_4$ . Cell sizes predicted by this technique are usually valid only for mixtures with compositions that are similar to that of the matching point.

In an attempt to make this simple technique more reliable, we originally proposed (Lee et al. 1982; Shepherd and Roller 1982) that  $A = A(\phi)$ . A preliminary assessment at that time indicated that this approach was viable for  $CO_2$  dilution of  $H_2$ -air mixtures. However, it is clear that this method is also limited since even equilibrium (CJ) detonation parameters are not universal functions of  $\phi$ . It does have the advantage that  $\phi$  is the most accessible nondimensional parameter and, as shown below, can provide a useful, fuel-specific correlation. In order to determine  $A(\phi)$ , measured values of  $\lambda$  and corresponding computed values of  $\Delta$  are used to calculate  $A$  from the definition  $A = \lambda/\Delta$ .

Results for  $A_2$  are shown in Fig. 7; these were computed from the  $H_2$ -air data shown in Fig. 4. Note the large variation in  $A$  with  $\phi$  and the maxima occurring near  $\phi = 0.7$  and  $\phi = 3.0$ . The unusual shape of this curve is similar to the effective activation energy curve and suggests that the variation in  $A$  may be due to the change in kinetic mechanism near the lean and rich limits.  $A_2(\phi)$  also drops rapidly at the extremes of the equivalence ratio range. This effect may be due to difficulties in the measurement, since the detonations are near the single-head spin limit (Moen et al. 1981) for these cases, or this may just reflect further changes in the kinetic mechanism. Behavior similar to that shown in Fig. 7 is also observed for the coefficients  $A_1$  and  $A_4$ . For the two lengths characteristic of the total reaction zone length,  $\Delta_3$  and  $\Delta_5$ , the coefficients  $A$  have a much smoother dependence on  $\phi$ .

What is the best choice for a reaction zone length? To determine this, the correlation between calculated reaction zone length

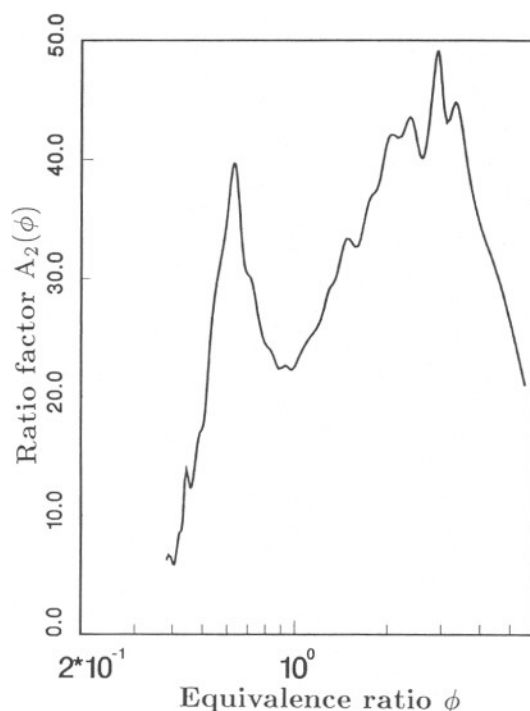


Fig. 7 Ratio  $A_2(\phi)$  of cell size  $\lambda$  to reaction zone length  $\Delta_2$  for  $H_2$ -air detonations (standard initial conditions).

and measured cell size has been tested for  $H_2$ -air and  $H_2$ -air- $CO_2$  detonations. The relations  $\lambda = A\Delta$  and  $\lambda = A(\phi)\Delta$  were both examined. Lacking quantitative estimates of the uncertainty in  $\lambda$ , correlations were judged purely on the appearance of data vs prediction plots. In general, all reaction zone lengths, scaled by a constant  $A_i$ , reproduce the general features of the  $\lambda$  vs  $\phi$  curve shown in Fig. 4. If a deviation of  $\pm 200\%$  between predicted and measured cell size is acceptable, any one of the lengths could be used for correlation with  $\lambda$ .

A more critical appraisal suggests that a  $\pm 50\%$  deviation may be achieved once  $A_i(\phi)$  has been estimated from a selected set of data. This is the approach I have taken to model the effect of diluents and changes in the initial conditions. The length  $\Delta_2$  (which is based on the location of Mach number 0.75) and the coefficient  $A_2$  shown in Fig. 7 were used for the predictions given below. The choice of  $\Delta_2$  and  $A_2$  for modeling is certainly not definitive, since this evaluation has been quite subjective. Other researchers may find different length scales more appealing and potentially more useful for predicting cell size. However, I feel that until substantial improvements are made in the experimental technique of cell size interpretation for

irregular cellular structures, more elaborate correlations cannot be justified. Efforts in this direction are in progress at Sandia Laboratories using digital image-processing techniques for interpretation of smoked foils.

What is the future of the empirical approach? Obviously, the simplicity of this technique and the development of oxidation mechanisms for the major fuel systems insures continued use for hazard analyses concerned with the detonability of gaseous mixtures. However, the complex and nonlinear interactions between fluid dynamics and chemistry that are actually occurring are simply being ignored. This serious deficiency and the quantitative inaccuracy of the simple correlations are sufficient reason to pursue a deeper understanding of this problem. In the interim, all predictions of this type should be used with caution and experimental data are to be preferred whenever possible. Development of a sound scientific basis for cell size prediction will hopefully make obsolete the ad hoc methods presently being used. On the other hand, the experimental problem of interpreting smoked foils and assigning a single characteristic cell size should not be underestimated.

### H<sub>2</sub>-Air-Diluent Detonations

#### CO<sub>2</sub> Dilution

Cell sizes have been measured both at McGill University (Guirao et al. 1982) and SNLA (Tieszen et al. 1985) for H<sub>2</sub>-air mixtures diluted with 5%, 10%, and 15% CO<sub>2</sub>. All mixtures were nominally at a total initial pressure of 1 atm and temperature of 298 K. Using the methodology described above, the cell sizes were predicted from the reaction zone lengths  $\Delta_2$  and the coefficient  $A_2$  shown in Fig. 7. Predictions and data are shown together in Fig. 8. Note that only a finite number of theoretical points are computed; the spline interpolation to those points is what is plotted in all figures. The agreement between predicted and measured cell size is fairly good, considering that repeated tests indicate that the uncertainty in the cell size can be 50%-100% or even higher for the largest cells measured.

The dramatic increase in cell size with relatively small amounts of dilution indicates the effectiveness of CO<sub>2</sub> as a detonation inhibitor. This effect has also been observed for hydrocarbon-air detonations by Moen et al. (1984b). The mechanism of inhibition by



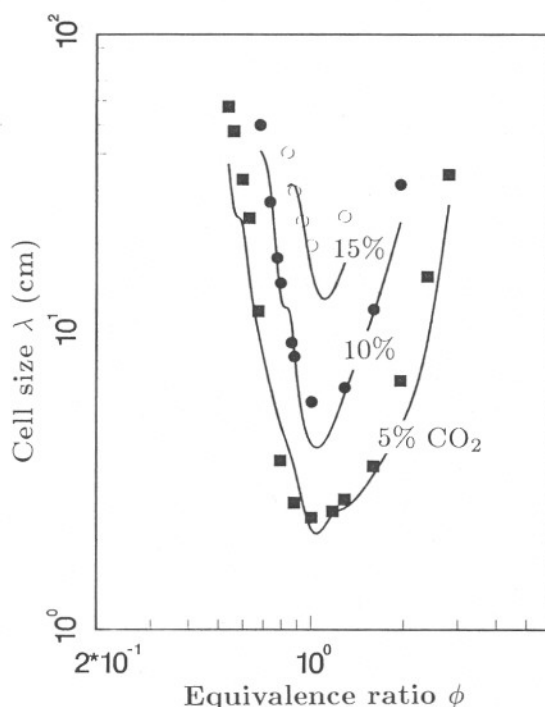


Fig. 8 Measured and predicted cell sizes for detonations in  $\text{H}_2$ -air- $\text{CO}_2$  mixtures (standard initial conditions).

dilution with relatively inert gases such as  $\text{CO}_2$  is primarily thermal in nature. That is, if addition of the diluent causes an increase in heat capacity then there will be a corresponding decrease in the detonation Mach number. This causes a decrease in the postshock temperature and pressure, which reduces the reaction rates, resulting in longer reaction zone lengths and increased cell size. Monatomic species such as Ar and He reverse this rule. For those diluents, the heat capacity decreases and the postshock temperature actually increases with increasing dilution until a substantial amount (greater than 50%) of diluent has been added.

In addition to this thermal effect, the diluent may actively participate in or enhance the rates of some reactions. This will be referred to as a chemical effect. An example of a chemical effect is the enhancement of the rate of reaction 5 by a factor of 20 when  $\text{H}_2\text{O}$  is the diluent.

Besides these two primary effects of diluents, a secondary effect can occur as a result of the thermal effect. Small amounts of polyatomic inert diluents can cause sufficient changes in postshock thermodynamic conditions that there is a change in rate-controlling

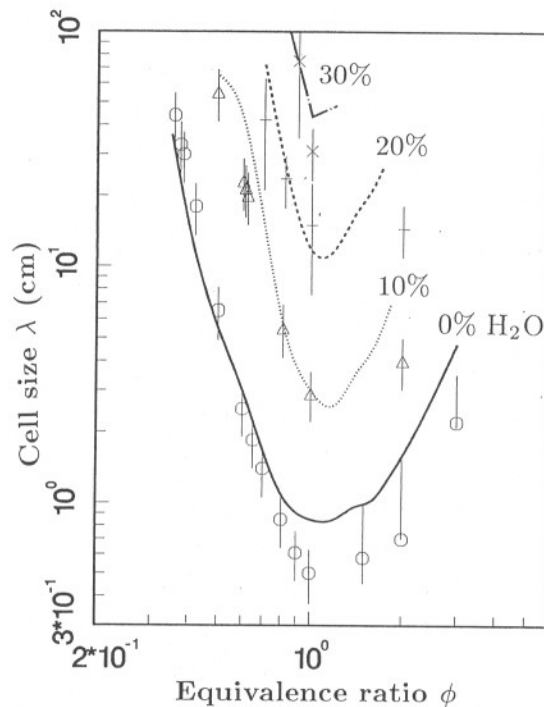


Fig. 9 Measured and predicted cell sizes for detonations in  $\text{H}_2$ -air- $\text{H}_2\text{O}$  mixtures. Nominal initial temperature of 373 K and fixed initial air density of 41.6 moles/ $\text{m}^3$ .

reaction. This is identical to the phenomenon described above in connection with the question of an intrinsic limit for  $\text{H}_2$ -air detonations. The same cautions about using global reaction rate expressions to extrapolate cell size also apply here.

### $\text{H}_2\text{O}$ Dilution

Cell sizes have been measured at SNLA (Tieszen et al. 1985) for hot  $\text{H}_2$ -air mixtures diluted with 0%, 10%, 20%, and 30% water vapor ( $\text{H}_2\text{O}$ ). The initial conditions for these experiments were representative of those that might occur during hypothetical accidents in nuclear powerplants. The mixtures were all heated to a nominal temperature of 373 K and the partial density of air was fixed at a value of 41.6 moles/ $\text{m}^3$ , the value at 298.15 K and 1 atm. This means that for each equivalence ratio and  $\text{H}_2\text{O}$  mole fraction, the initial pressure was different. The model predictions are therefore being tested in several ways simultaneously. The effects of initial temperature, pressure, and dilution are all present in each of these tests. Further consideration of the effect of separately varying each of the initial conditions will be made below.

Data and predictions are shown together in Fig. 9. Uncertainty estimates in the measured cell size are also shown for each datum. The predictions are again in fair agreement with the data. Disagreement outside the uncertainty bounds should be noted for the 0% case near stoichiometric composition and for the 10% and 20% cases on the rich side. Comparison with the H<sub>2</sub>-air data of Fig. 4 reveals that the cell size at a given value of  $\phi$  is smaller for the 0% case at 373 K than for the room temperature and pressure case. As discussed below, the calculations indicate that this is due to the higher density of the hot cases rather than the increased temperature.

As pointed out by Westbrook and Urtiew (1982), increasing the initial temperature at a fixed initial pressure increases rather than decreases the reaction zone length. This is due to the decrease in reactant density when the initial temperature is increased at fixed initial pressure. The decrease in reactant density causes a decrease in reaction rates and, therefore, a longer reaction zone. The VN temperature does slightly increase with increasing initial temperature, which will tend to decrease the reaction zone length. However, that effect is much weaker than the density effect. If the initial mixture density is held constant (as in the SNLA H<sub>2</sub>-air-H<sub>2</sub>O tests) or increases as the initial temperature is increased, the model predicts that the reaction zone becomes shorter.

### Thermal vs Chemical Effects

What is the exact mechanism of reaction inhibition by CO<sub>2</sub> and H<sub>2</sub>O? In order to address this question, some additional computations have been performed so that the two diluents can be compared on an equal basis. To remove the temperature and pressure effects present in the H<sub>2</sub>O tests discussed above, reaction zone lengths have been computed for the artificial case of H<sub>2</sub>-air-H<sub>2</sub>O mixtures at a constant initial pressure of 1 atm and initial temperature of 298 K. The results for stoichiometric mixtures at these standard initial conditions are shown in Fig. 10 as a function of diluent mole fraction. For comparison, the results for N<sub>2</sub> dilution are also shown.

Both H<sub>2</sub>O and CO<sub>2</sub> have very similar effects and are much more effective than N<sub>2</sub> as inhibitors. This is primarily due to the difference in the heat capacity of the triatomic and diatomic molecules, the thermal effect discussed above, although there is also a pronounced

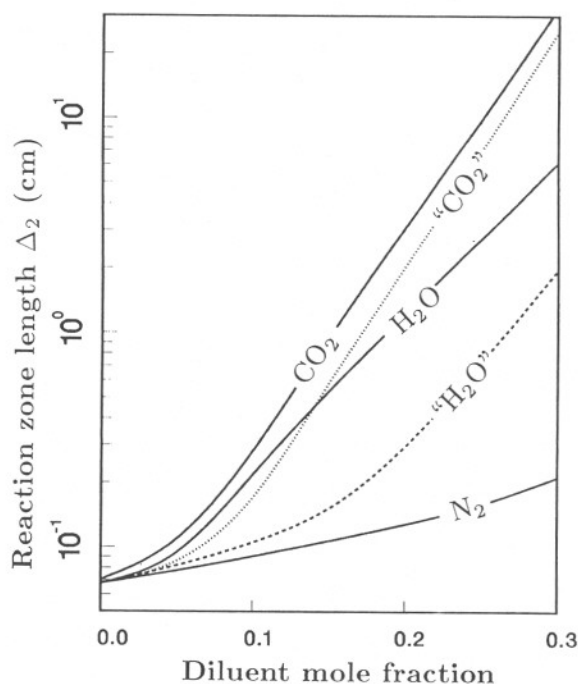


Fig. 10 Reaction zone length  $\Delta_2$  for  $\text{CO}_2$ ,  $\text{H}_2\text{O}$ , and  $\text{N}_2$  dilution of stoichiometric mixtures of  $\text{H}_2$ -air at standard initial conditions. The curves labeled " $\text{CO}_2$ " and " $\text{H}_2\text{O}$ " are for artificially inert but thermodynamically identical diluents.

chemical effect in the case of  $\text{H}_2\text{O}$ . This chemical effect can be seen clearly by repeating the computations with artificial diluents that have identical thermodynamic properties as the actual species but are chemically inert. That is, the artificial diluents do not participate in any reactions except as a third-body with the efficiency of Ar.

The results of these calculations are also shown in Fig. 10 as the curves labeled " $\text{H}_2\text{O}$ " and " $\text{CO}_2$ ". The chemical effect of  $\text{CO}_2$  is seen to be quite small. This may not be the case for rich mixtures since substantial amounts of CO will be produced (less than 1% of the  $\text{CO}_2$  is converted to CO for stoichiometric mixtures) and the CO will compete for the OH radical through reaction 22. The chemical effect of  $\text{H}_2\text{O}$  is much stronger. This is primarily due to the very large efficiency of  $\text{H}_2\text{O}$  in the three-body reaction 5. The effect is most pronounced for greater than 10% diluent. This threshold is indicative of the change in the thermodynamic state required to change the rate-limiting reaction step.

A clearer picture of the relation between thermal and chemical effects can be obtained by plotting the postshock temperature vs

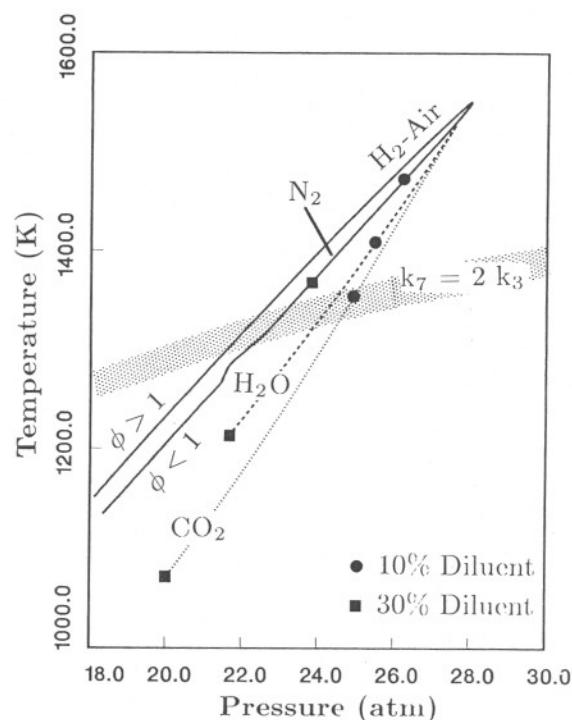


Fig. 11 Comparison of the postshock pressure and temperature states of  $\text{H}_2$ -air detonations and stoichiometric  $\text{H}_2$ -air mixtures diluted with  $\text{CO}_2$ ,  $\text{H}_2\text{O}$ , and  $\text{N}_2$ . Standard initial conditions.

pressure for both the undiluted  $\text{H}_2$ -air and the diluted stoichiometric cases shown in Fig. 10. This is done in Fig. 11. A similar comparison has been made by Takai et al. (1974) for  $\text{H}_2$ - $\text{O}_2$  mixtures diluted with Ar, He,  $\text{N}_2$ , and  $\text{CO}_2$ . Note that the  $\text{N}_2$  curve is indistinguishable from the lean branch of the  $\text{H}_2$ -air curve, indicating that the thermal effect of  $\text{N}_2$  is almost identical to the substitution of  $\text{O}_2$  for  $\text{H}_2$ . That the chemical effect of  $\text{N}_2$  is negligible can be verified by comparing the computed reaction zone lengths to those of  $\text{H}_2$ -air at similar VN states.

The  $\text{CO}_2$  and  $\text{H}_2\text{O}$  curves are separated because of the difference in the molecular weight of the two molecules. The rich and lean branches of the  $\text{H}_2$ -air curve are separated for similar reasons: The addition of  $\text{H}_2$  causes a continuous decrease in initial molecular weight of the mixture. The main point of Fig. 11 is in the relation of the  $(T_{\text{vn}}, P_{\text{vn}})$  loci to the shaded band labeled  $k_7 = 2 k_3$ . This band represents the approximate location of the change of rate-limiting reactions, the criterion used is the same as in the classical second limit discussions. This criterion is that the rate of reaction 7 is



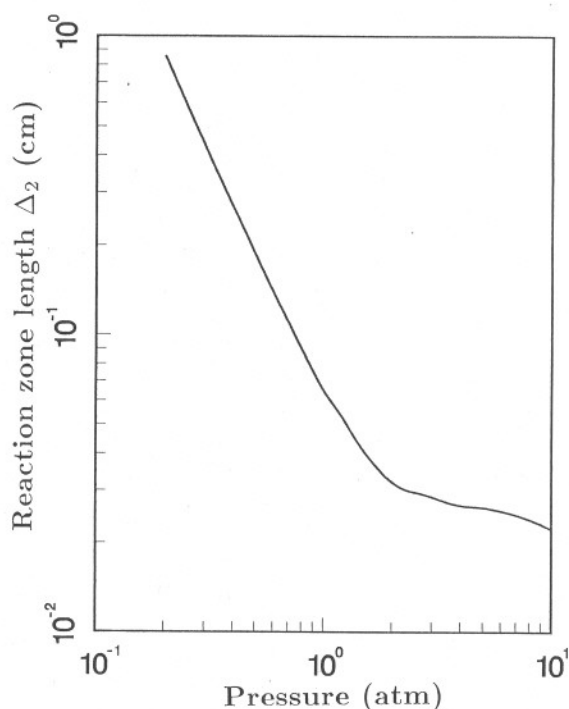


Fig. 12 Pressure dependence of reaction zone length  $\Delta_2$  for stoichiometric  $H_2$ -air mixtures at standard initial temperature.

twice that of reaction 3, i.e.,  $k_7 = 2 k_3$ . This relation conveniently reduces to a  $P_{vn} - T_{vn}$  relation if the diluent concentration is fixed. Above the shaded band, the standard H-OH-O chain-branching reaction mechanism dominates; below, the alternative H-HO<sub>2</sub>-H<sub>2</sub>O<sub>2</sub>-OH mechanism is most important. Note that the CO<sub>2</sub> and H<sub>2</sub>O loci cross the shaded band at relatively low diluent concentrations. This indicates that the effective activation energy change will be important in predicting the dilution experiments discussed above. This is where a simple global reaction time expression will fail. The shaded band also crosses the H<sub>2</sub>-air locus at the equivalence ratio range where the beginning of the change in the effective activation energy occurs.

#### Effect of Initial Conditions

As pointed out above, the H<sub>2</sub>O dilution experiments involve simultaneous changes in the initial conditions. Westbrook and Urtiew (1982) have considered these changes independently, but there is an additional interaction that occurs when pressure and temperature are both changed simultaneously. Westbrook and Urtiew (1982) have shown that the pressure dependence of H<sub>2</sub>-air reaction zone

lengths at fixed initial temperature has a strong change in character between 1 and 10 atm. As shown in Fig. 12, below 1 atm the pressure dependence can be described by  $p^n$ , where  $n \approx -1.5$ . The exponent  $n$  increases with increasing initial pressure and appears to go to change sign at about 3 atm. This is, in fact, another manifestation of the change in reaction mechanism. Referring to Fig. 11, we can see that an increase in the initial pressure (which leaves  $T_{vn}$  essentially unchanged) will shift the  $P_{vn} - T_{vn}$  locus to the right and eventually beneath the shaded band, thus yielding the mechanism change.

This mechanism change feeds back into the temperature effect so that at low pressure, an increase of temperature at fixed initial pressure will increase the reaction zone length and at high pressures will decrease the reaction zone length. This is shown in Fig. 13. The trade-off between the changing pressure exponent and the slightly increasing postshock temperature produces this effect. An experimental test of the effect is shown in Fig. 14, where experimental cell sizes and predictions are compared for constant-pressure and

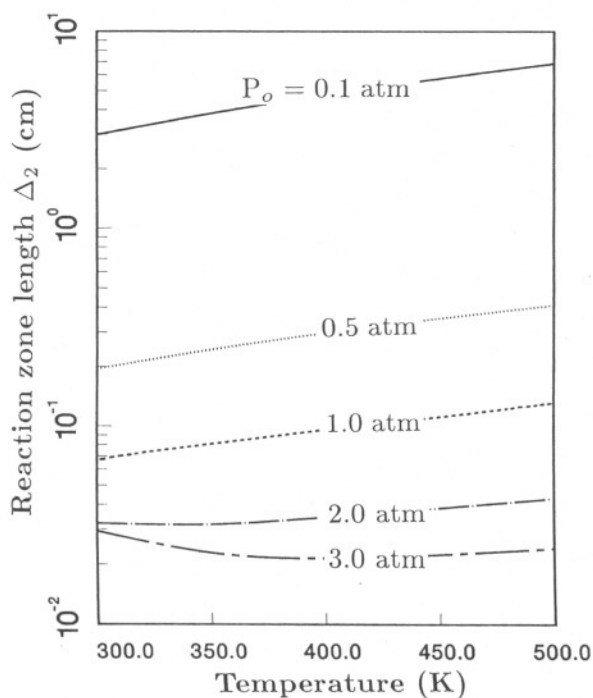


Fig. 13 Temperature dependence of reaction zone length  $\Delta_2$  for stoichiometric mixtures of  $H_2$ -air at pressures of 0.1, 0.5, 1.0, 2.0, and 3.0 atm.

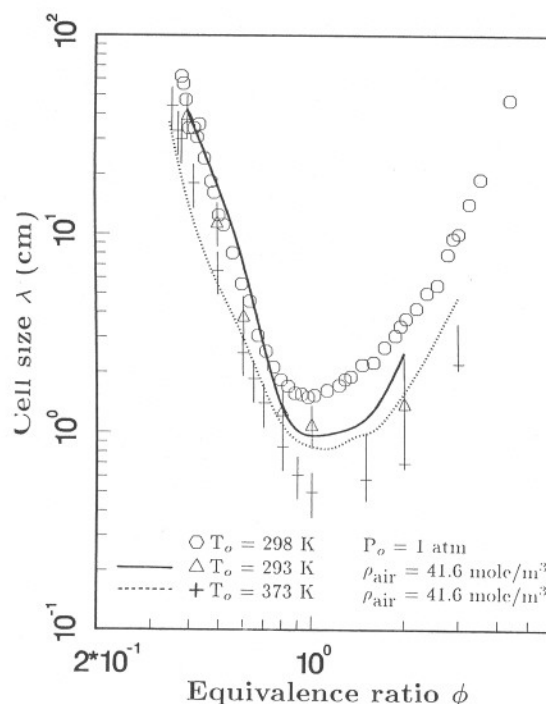


Fig. 14 Measured and predicted cell sizes for  $H_2$ -air detonations. Initial conditions are: i) Constant pressure of 1 atm and temperature of 298 K; ii) Constant air density of  $41.6 \text{ mole/m}^3$  and initial temperature of 293 K; iii) Constant air density of  $41.6 \text{ mole/m}^3$  and initial temperature of 373 K.

constant air density initial conditions at 298 K, and constant air density cases at 373 K. The agreement between theory and prediction is again fair.

Additional computations demonstrate that if the equivalence ratio is made sufficiently small or large, i.e. for very lean or very rich mixtures, the reaction zone length will decrease with increasing initial temperature at fixed initial pressure. These changes in direction of the temperature effect also correspond to the postshock thermodynamic state moving below the shaded band in Fig. 11. All of these temperature and pressure effects can be viewed as a manifestations of the change in kinetic mechanism and demonstrate the importance of detailed kinetic modeling in understanding these phenomena.

### Summary

The possibility of using detailed kinetic calculations and simple correlations to predict the detonation cell size for  $H_2$ -air-diluent

detonations has been explored. A review of the existing theoretical models for cell size prediction indicates that an appropriate theory has still not been developed. Lacking a sound theoretical basis, a simple linear proportionality relationship has been used to correlate cell size to reaction zone lengths. Single parameter correlations are accurate only to within  $\pm 200\%$  over an equivalence ratio range of 0.38 to 5.56 for  $\text{H}_2$ -air mixtures initially at ambient conditions.

An improved correlation using existing data can predict within  $\pm 50\%$  the effects of dilution with  $\text{CO}_2$  or  $\text{H}_2\text{O}$  and the effects of simultaneously changing the initial conditions. The dramatic inhibition effect of  $\text{CO}_2$  and  $\text{H}_2\text{O}$  is explained in terms of both thermal and chemical effects and a secondary effect due to a switch in the rate limiting kinetic step. The existence of an intrinsic detonability limit is shown to be dubious although a pronounced change in the effective activation energy and reaction pathways is observed as the extremes of the equivalence ratio range are approached.

The effect on the reaction zone length due to changing initial conditions (temperature and pressure) is shown to be more complex than previously thought. Increasing the initial temperature at low initial pressures (less than 1 atm) causes an increase in the reaction zone length; the opposite occurs at higher initial pressures. This is another manifestation of the change in rate-controlling reactions due to a change in the thermodynamic state. These mechanism changes can make extrapolation of existing data with global mechanisms risky.

Further research is needed to place the prediction of cell size by simple kinetic models on a sound scientific basis. At the same time, further refinement of the experimental techniques of interpreting smoked foils is needed before substantial improvements in the correlation can be made. The observed multimode structure of ordinary fuel-air detonations suggests that the cellular structure might not be characterized by a single parameter that is uniquely related to an idealized reaction zone length.

#### Acknowledgment

I would like to thank J. H. Lee, R. Knystautas, and students at McGill University, as well as S. R. Tieszen, M. P. Sherman, and W. B. Benedick of SNLA, for generously sharing their data with me.

J. C. Cummings of SNLA provided valuable criticism and suggested the chemical effect computations. R. Strehlow originally pointed out to me the relevance of the extended 2nd-limit. This work was supported by the U.S. Nuclear Regulatory Commission and performed at Sandia National Laboratories which is operated for the U.S. Department of Energy under contract DE-AC04-76DP00789.

### References

- Atkinson, R., Bull, D.C., and Schuff, P.J. (1980) Initiation of spherical detonation in hydrogen/air. *Combustion and Flame* **39**, 287-300.
- Barthel, H.O. and Strehlow, R.A. (1966) Wave propagation in one-dimensional reactive flows. *Phys. Fluids* **9**, 1896-1907.
- Barthel, H.O. (1974) Predicted spacings in hydrogen-oxygen-argon detonations. *Phys. Fluids* **17**, 1547-1553.
- Belles, F.E. (1959) Detonability and chemical kinetics: Prediction of limits of detonability of hydrogen. *7th Symposium (International) on Combustion*, pp. 745-751. The Combustion Institute, Pittsburgh, Pa.
- Bull, D.C., Ellsworth, J.E. and Schuff, P.J. (1982) Detonation cell structure in fuel/air mixtures *Combust. and Flame* **45**, 7-22.
- Chiu, K.W. and Lee, J.H. (1976) A simplified version of the Barthel model for transverse wave spacings in gaseous detonation. *Combust. and Flame* **26**, 353-361.
- Erpenbeck, J.J. (1969) Theory of Detonation Stability. *12th Symposium (International) on Combustion*, pp. 711-721. The Combustion Institute, Pittsburgh, Pa.
- Fickett, W. and Wood, W.W. (1966) Flow calculations for pulsating one-dimensional detonations. *Phys. Fluids* **9**(5), 903-916.
- Gordon, S. and McBride, B.J. (1971) Computer program for the calculation of complex chemical equilibrium compositions, rocket performance, incident and ReFlected shocks and Chapman-Jouget detonations. NASA SP-273.
- Guirao, C.M., Knystautas, R., Lee, J.H., Benedick, W.B., and Berman, M. (1982) Hydrogen-air detonations. *19th Symposium (International) on Combustion*, pp. 583-590. The Combustion Institute, Pittsburgh, Pa.
- Howe, P., Frey, R., and Melani, G. (1976) Observations concerning transverse waves in solid explosives. *Combust. Sci. Technol.* **14**, 63-74.

- Lee, J.H. (1984), Parameters of gaseous detonation, *Ann. Rev. Fluid Mech.* **16**, 311-336.
- Lee, J.H., Knystautas, R.M., Guirao, C., Benedick, W.B. and Shepherd, J.E. (1982) Hydrogen-air detonations. *Proceedings of the Second International Workshop on Hydrogen Behavior in Light Water Reactors* (edited by M. Berman and L. Thompson), pp. 961-1006. SAND82-2456, Sandia National Laboratories, Albuquerque, N.M.
- Miller, J.A., Mitchell, R.E., Smooke, M.D., and Kee, R.J. (1982) Towards a comprehensive kinetic mechanism for oxidation of acetylene. *19th Symposium (International) on Combustion*, pp. 181-196. The Combustion Institute, Pittsburgh, Pa.
- Moen, I.O., Donato, M., Knystautas, R. and Lee, J.H. (1981) The influence of confinement on the propagation of detonations near the detonability limits. *18th Symposium (International) on Combustion*, pp. 1615-1622. The Combustion Institute, Pittsburgh, Pa.
- Moen, I.O., Funk, J.W., Ward, S.A., Rude, G.M. and Thibault, P.A. (1984a) Detonation length scales for fuel-air explosives. *AIAA Progress in Astronautics and Aeronautics* **94**, 55-79. AIAA, New York.
- Moen, I.O., Ward, S.A., Thibault, P.A., et al. (1984b) The influence of diluents and inhibitors on detonations. *20th Symposium (International) on Combustion* (to be published).
- Oran, E.S., Boris, J.P., Young, T., et al. (1982) Numerical simulations of detonations in hydrogen-air and methane-air mixtures. *18th Symposium (International) on Combustion*, pp. 1641-1649. The Combustion Institute, Pittsburgh, Pa.
- Shepherd, J.E. and Roller, S.F. (1982) Effect of steam on the detonability of hydrogen-air mixtures. *Proceedings of the Second International Workshop on Hydrogen Behavior in Light Water Reactors* (edited by M. Berman and L. Thompson), pp. 1007-1026. SAND82-2456, Sandia National Laboratories, Albuquerque, N. M.
- Shchelkin, K.I. and Troshin, Ya.K. (1965) *Gasdynamics of Detonations*. Mono Book Corp., Baltimore, Md.
- Strehlow, R.A. and Fernandes, F.D. (1965) Transverse waves in detonations. *Combust. and Flame* **9**, 109-119.
- Strehlow, R.A., Maurer, R.E., and Rajan, S. (1969a) Transverse waves in detonations: I. Spacing in the hydrogen-oxygen system. *AIAA J.* **7**, 323-328.
- Strehlow, R.A. and Engel, C.D. (1969b) Transverse waves in detonations: II. Structure and spacing in  $H_2-O_2$ ,  $C_2H_2-O_2$ ,  $C_2H_4-O_2$ , and  $CH_4-O_2$  systems. *AIAA J.* **7**, 492-496.



- Strehlow, R.A. (1969c) The nature of transverse waves in detonations. *Astronaut. Acta* **14**, 539-548.
- Takai, R., Yoneda, K., and Hikata, T. (1974) Study of detonation wave structure. *15th Symposium (International) on Combustion*, pp. 69-78. The Combustion Institute, Pittsburgh, Pa.
- Taki, S. and Fujiwara, T. (1982) Numerical simulations of triple shock behavior of gaseous detonation. *18th Symposium (International) on Combustion*, pp. 1671-1681. The Combustion Institute, Pittsburgh, Pa.
- Tieszen, S.R., Sherman, M.P., Benedick, W.B., et al. (1985) Detonation cell size measurements in  $H_2$ -air- $H_2O$  mixtures. 10th International Colloquium on Dynamics of Explosions and Reactive Systems.
- Vasiliev, A.A. and Nikolaev, Yu. (1978) Closed model of a detonation cell. *Acta Astronaut.* **5**, 983-996.
- Warnatz, J. (1984) Rate coefficients in the C/H/O system. *Combustion Chemistry* (edited by W.C. Gardiner). Springer, N.Y.
- Westbrook, C.K. and Urtiew, P.A. (1982) Chemical kinetic prediction of critical parameters in gaseous detonations. *19th Symposium (International) on Combustion*, pp. 615-623. The Combustion Institute, Pittsburgh, Pa.
- Westbrook, C.K. (1982) Hydrogen oxidation kinetics in gaseous detonations. *Combust. Sci. Technol.* **29**, 65-79.
- Westbrook, C.K. and Urtiew, P.A. (1983) Use of chemical kinetics to predict critical parameters of gaseous detonation. *Fiz. Goreniya Vzryva* **19**(6), 65-76.
- Westbrook, C.K. and Dryer, F.L. (1984) Kinetic modeling of hydrocarbon combustion. *Prog. Energy Combust. Sci.* **10**, 1-57.